Research on Engineering Structures & Materials
www.jresm.org

Research Article

Stress analysis and safety assessment of long-span prestressed concrete continuous girder bridge based on bridge jacking technology and construction monitoring

Ping Guo [*,a]

Railway Engineering School, Liuzhou Railway Vocational Technical College, Liuzhou, 545616, China

Article Info

Article History:

Received 29 Jul 2026

Accepted 26 Sep 2026

Keywords:

Bridge jacking;
Construction monitoring;
Concrete continuous girder bridge;
Stress analysis;
Safety assessment

Abstract

Bridge jacking is a complex mechanical process that must be combined with strict construction monitoring to ensure structural safety. To explore the structural stress mechanism and safety status of a large-span prestressed concrete continuous girder bridge during the jacking construction process, this study is based on a three-span prestressed concrete continuous box girder bridge, based on hydraulic synchronous lifting technology and high-precision construction monitoring means. It arranges vibrating wire strain gauges and displacement sensors on the pier top section, mid-span section and side span section to obtain real-time monitoring data of the entire jacking process. The research results showed that the stress increment at the bottom plate compressive stress measuring point on the pier top section showed a good linear growth with the jacking amount, while the stress increment at the mid-span bottom plate tensile stress measuring point showed non-linear growth characteristics. In terms of safety assessment, the safety factors of the most unfavorable tensile stress measuring points were all 1.45, which was higher than the safety reserve threshold of 1.2. The safety factors of the compressive stress measuring points reached 2.72~16.80, and the maximum displacement synchronization error of 0.26 mm was far less than the specification limit of 1.5 mm. The results show that during the jacking process, the compressive stress response of the pier top section is the most significant and linearly stable, and the structure is always in an elastic working state. This research provides reliable technical reference and theoretical basis for the safety control of long-span bridge jacking construction.

© 2026 MIM Research Group. All rights reserved.

1. Introduction

Due to the rapid development of the national transportation infrastructure, many prestressed concrete continuous girder bridges that were constructed in the past have encountered issues like settling of the beams, aging of the supports, and inadequate clearance beneath the bridges after decades of use. These issues have seriously affected the normal use function and driving safety of the bridge [1-2]. The traditional demolition and reconstruction method is not only costly and long-term, but also causes traffic interruption and waste of resources, making it difficult to meet the requirements of modern society for sustainable operation of infrastructure. Bridge jacking technology is an active and efficient means of structural maintenance and renovation. It uses a hydraulic synchronization system to lift the upper structure as a whole, and can complete support replacement, linear adjustment or clearance modification without dismantling the bridge. It has been utilized more frequently in bridge repair and maintenance operations both domestically and internationally in recent years [3-4].

*Corresponding author: guo_gping@outlook.com
[a]orcid.org/0009-0002-0503-718X
DOI: http://dx.doi.org/10.17515/resm2026-2071im0729rs

Long-span prestressed concrete continuous girder bridge jacking is currently a common use for computer-controlled hydraulic synchronous lifting technology. To create a closed-loop control system, this method places several jacks on top of the pier and uses a central controller to gather pressure and displacement signals in real time. Theoretically, it can control the lifting displacement error of each fulcrum within the range of millimeters. However, long-span prestressed concrete continuous girder bridges are high-order statically indeterminate structures with large overall weight, high structural stiffness, and extremely sensitive to uneven displacements [5]. During the jacking process (JP), even a small difference in fulcrum displacement will cause significant internal force redistribution, which may lead to serious consequences such as concrete cracking in the negative moment area of the pier top, excessive tensile stress (TS) in the mid-span positive moment area, and even damage to the beam [6]. Therefore, it is difficult to fully ensure structural safety by relying solely on the synchronous control accuracy of the jacking system. It must be combined with strict construction monitoring to capture the stress response of the structure in real time to achieve safe control of the entire JP.

At this stage, Nishio H proposed a three-dimensional finite element prestressed tension and anchorage analysis method in view of the current situation that the traditional initial stress method had insufficient analysis accuracy and could not calculate the impact of anchorage loss in large-scale, high-order ultra-statically indeterminate prestressed concrete structures. The outcomes revealed that this method could effectively calculate the anchorage loss effect and ensure that the prestressed concrete structure after construction met the design objectives [7]. Zhang Z et al. addressed the technical challenges in the jacking and reconstruction of urban continuous bridges with huge tonnage, high longitudinal slopes, and high piers by proposing a construction process analysis approach that integrates finite element analysis and on-site testing. The results showed that the proposed construction technology could effectively solve the jacking problem, and the internal force changes during uneven jacking were evaluated through structural analysis [8]. Gao H et al. proposed an overall synchronous jacking design scheme that comprehensively considered jacking height, jacking form, slope adjustment method, and weight in view of the current situation that it was difficult to raise the bridge elevation in the jacking and reconstruction project of concrete continuous box girder bridges. The results verified the rationality of the jacking plan through the comparison of real-time monitoring data and theoretical values. This provided a technical reference for similar concrete bridge jacking and reconstruction projects [9]. In light of the current situation, where the structure does not form an integral system during the jacking construction of long-span steel box girders and the risk of slippage and overturning under wind load increases significantly, Tian Q et al. proposed a wind-friction coupling model based on three-dimensional finite element analysis and static wind three-force theory. According to the findings, the main beam's equivalent stress reached 155 MPa, and the guide beam's 60-meter cantilever stage was the least advantageous working condition [10].

While the aforementioned studies yielded favorable experimental outcomes, the processing of monitoring data frequently overlooked false strains induced by temperature variations. The thermal inertia of concrete structures results in significant differences between the internal temperature field and the ambient temperature. If no correction is made, it will directly affect the accuracy of stress analysis [11-12]. For long-span prestressed concrete continuous girder bridges utilizing bridge jacking technology and construction monitoring, this study suggests a stress analysis and safety assessment approach. Among them, the stress analysis uses vibrating wire strain gauges and displacement sensors arranged on the pier top section, mid-span section (MSS) and side span section to obtain real-time monitoring data of the entire JP. This reveals the variation pattern of key section stress with jacking amount and the strain distribution characteristics along the beam height. Safety assessment is based on stress safety factor, displacement synchronization error and other indicators to establish a comprehensive safety assessment system to achieve quantitative identification and graded early warning of the structural safety status during the entire JP. This study obtains real-time monitoring data of the entire JP through vibrating wire strain gauges and displacement sensors arranged on the pier top section, MSS, and side span section. This can reveal the change pattern of key section stress with jacking amount and the strain distribution characteristics along the beam height. The innovation of this research lies in proposing a

comprehensive methodological framework for safety monitoring and assessment specifically tailored for long-span prestressed concrete continuous girder bridges during jacking. This framework systematically integrates multi-source information, including stress distribution along the beam height, on-site temperature correction, stress safety factors, and displacement synchronization errors, while establishing a graded warning criterion based on the most unfavorable indicators. Although the specific numerical findings are case-dependent, the sensor layout principles, temperature correction procedures, and safety classification standards embedded in this framework are systematically transferable, providing a methodological reference for safety control in similar bridge jacking projects.

Compared with existing studies, the potential academic contributions of this research are as follows: (1) It fills the gap in the quantitative evidence of temperature correction in the monitoring of uplift construction. (2) It reveals the differentiated growth patterns of stress responses in the directly affected area (at the pier top) and the indirectly affected area (at the mid-span), providing a theoretical basis for the optimization of measurement points and the prediction of risk zones.

2. Methods and Materials

2.1 Engineering Overview

The bridge under investigation in this study is a three-span prestressed concrete continuous box girder bridge with a span arrangement of 80 m+130 m+80 m. It was constructed in 2004 and has been in service for approximately 22 years. Due to long-term service, the bridge has experienced support aging and insufficient under-bridge clearance, which seriously affects normal traffic safety. Therefore, the integral hydraulic synchronous jacking technology is adopted to lift the superstructure by a target elevation of 200 mm without demolishing the bridge. The original bearings are pot rubber bearings. During the jacking construction process, the bridge is fully closed to traffic, and the load conditions only consider the dead load (self-weight) and secondary dead load (pavement and parapets), without considering live loads. The temporary support system adopts steel cushion blocks, and four 200t hydraulic jacks are arranged at each jacking pier. The two-dimensional elevation layout and cross-sectional dimensions of the bridge are shown in Figure 1.

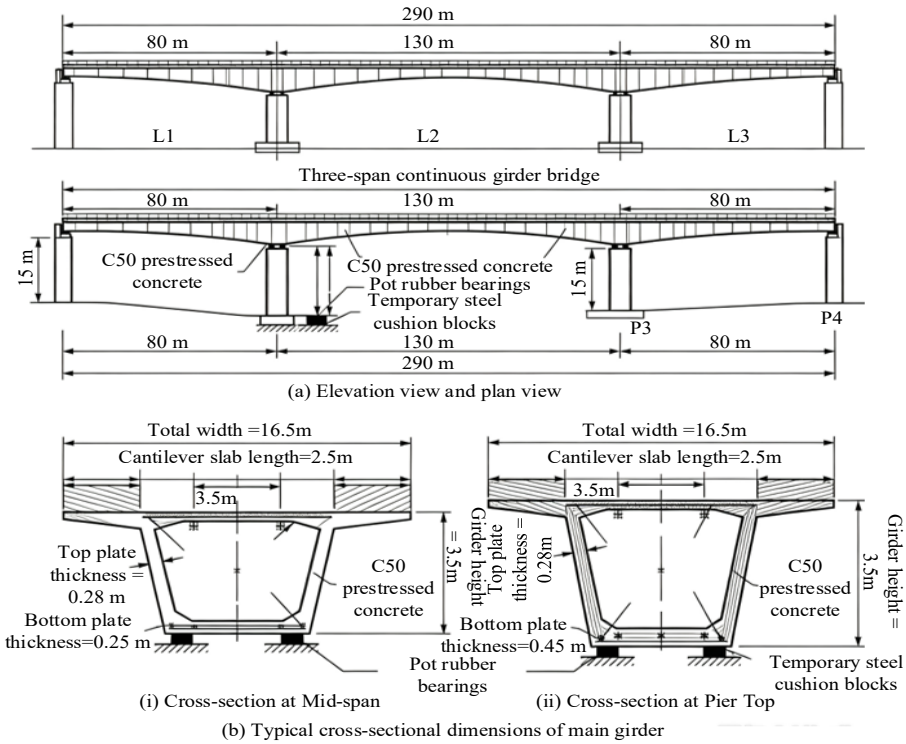


Fig. 1. Plan view and cross-sectional dimensions of the bridge layout

2.2 Bridge Jacking Construction Technology and Monitoring Plan

Bridge jacking is a complex mechanical process, so strict construction monitoring must be combined during the jacking implementation process. The study first elaborates on the technical details of synchronous jacking of long-span bridges, as well as the monitoring scheme for key section stress, displacement and other parameters. This can provide a basis for theoretical analysis of models and assessment of structural safety. Large-span prestressed concrete continuous girder bridges are extremely sensitive to uneven displacement due to their large total weight and high structural stiffness [13-14]. Therefore, the lifting system must use computer-controlled hydraulic synchronous lifting technology. Its core components include hydraulic pump station, jack, displacement sensor, pressure sensor and central controller, forming a closed-loop control system. The relevant diagram is shown in Figure 2.

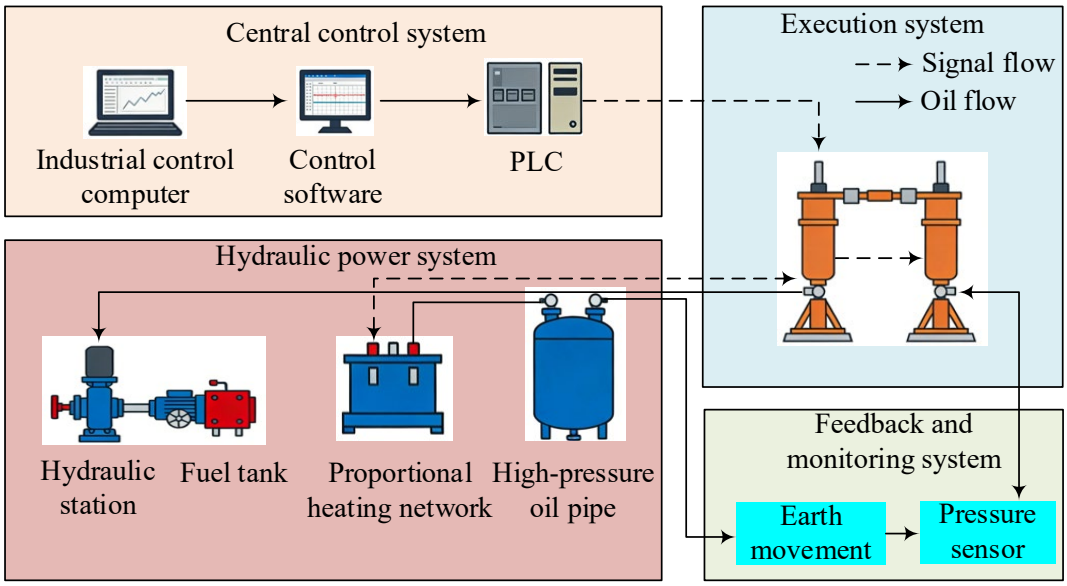


Fig. 2. Hydraulic synchronous lifting system schematic diagram

In Figure 2, the determination of the lifting force is the basis of the scheme design. Theoretically, the required total jacking force F_{total} should be less than the sum of the dead load reaction forces of the bridge, taking into account the second-stage dead load and possible over-top reserves. The relevant mathematical expression is shown in Equation (1).

$$F_{total} = k \cdot \sum_{i=1}^{n} R_{gi} \tag{1}$$

In Equation (1), R_{gi} represents the dead load reaction force of the ith fulcrum. n indicates the quantity of supports involved in jacking. k represents the safety factor, which is used to overcome static friction resistance and ensure a smooth JP. In addition, the additional lifting force F_{rated} of each jack needs to satisfy the constraints shown in Equation (2).

$$F_{rated} \geq \frac{F_{total}}{m} \cdot \gamma \tag{2}$$

In Equation (2), m represents the number of jacks, and γ represents the uneven coefficient. During the actual jacking operation, the measured hydraulic pressure for each 200t jack ranged from 12.5 MPa to 18.2 MPa, corresponding to actual lifting loads of 98 kN to 143 kN per jack, with a total jacking force of approximately 1,920 kN under the 20 mm jacking condition. These values are within the rated capacity with a sufficient safety margin. The size of the piers, the placement of the supports, and the temporary support system must all be taken into consideration while designing the jack plan. During the project, four 200t hydraulic jacks are arranged symmetrically on the top of each lifting pier along the cross-bridge direction, and reliable temporary steel supports are set up for protection. In synchronous jacking technology, its core lies in displacement synchronization and load balance. That is, the control system adopts a strategy of displacement closed-loop control

as the main part and pressure closed-loop control as the supplement. The displacement error Δ_{error} during the JP must be strictly controlled within the allowable range to prevent the beam from cracking. The relevant mathematical expression is shown in Equation (3).

$$|\Delta_{error}| = |\varphi_i - \varphi_j| \leq [\Delta] \tag{3}$$

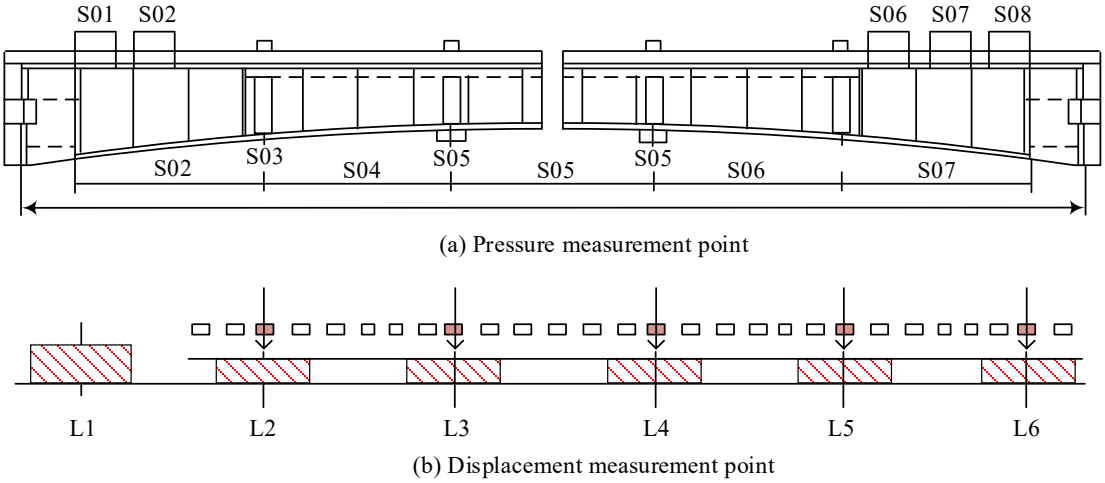
In Equation (3), φ_i and φ_j display the actual jacking displacement of adjacent fulcrums respectively. $[\Delta]$ represents the allowable displacement difference. The purpose of construction monitoring is to capture the evolution of the structure's internal forces during the JP and prevent irreversible damage to the structure. The monitoring content mainly includes concrete strain, structural displacement, and temperature field of key sections. First, in terms of the layout of stress measurement points, vibrating wire strain gauges are used for stress monitoring. It has the advantage of directly measuring frequency and converting it into strain [15-16]. Among them, the strain measured by the vibrating wire strain gauge is the total strain ε_{total} of concrete, and the temperature effect and non-stress strain need to be deducted. The mathematical expression of the mechanical strain ε_{mech} actually used in stress analysis is shown in Equation (4).

$$\varepsilon_{mech} = \varepsilon_{total} - \varepsilon_T - \varepsilon_{sh} \tag{4}$$

In Equation (4), ε_T represents the temperature strain, and ε_{sh} represents the concrete shrinkage strain. The stress σ_c of concrete can be calculated by Equation (5).

$$\sigma_c = E_c \cdot (\varepsilon_{mech}^{t} - \varepsilon_{mech}^{t0}) \tag{5}$$

In Equation (5), ε_{mech}^{t0} represents the initial mechanical strain before the start of jacking. Displacement monitoring includes jacking displacement and overall structural deformation. High-precision displacement sensors were arranged at each jacking point to directly measure the jack stroke. Additionally, precision levels or total stations are arranged at key locations in the middle and side spans of the main span to monitor the impact of jacking on adjacent spans. Figure 3 depicts the arrangement of stress and displacement measurement sites.



(a) Pressure measurement point

(b) Displacement measurement point

Fig. 3. Schematic diagram of stress and displacement measurement points layout

Figure 3 displays the location of the stress and displacement measuring points (MPs) on the bridge facade. Finally, temperature changes are the most important source of interference in strain measurements. To eliminate the influence of temperature, this study first sets up temperature compensation blocks at the same cross-section position of the bridge and pasted compensation strain gauges. Meanwhile, a temperature sensor is buried to record the temperature gradient inside the beam. The actual stress correction can be based on the material thermal expansion coefficient, and the relevant mathematical expression is shown in Equation (6).

$$\sigma_{corrected} = E_c \cdot (\varepsilon_m - \alpha \cdot \Delta T) \tag{6}$$

In Equation (6), ΔT represents the temperature change relative to the reference moment, and E_c represents the elastic modulus of concrete. The temperature measurement uncertainty is ±0.1°C for the PT100 sensors, resulting in a maximum strain measurement error of approximately ±1.2 με

after temperature correction, which is negligible compared with the measured strain variations. If the temperature difference increases, the thermal correction term would grow proportionally, and larger thermal gradients may induce additional TS in the concrete, potentially reducing the safety margin. Nevertheless, the correction formulas remain valid as long as the concrete stays in the elastic range without thermal cracking. Six temperature compensation blocks (150 mm × 150 mm × 300 mm, same C50 concrete) are placed at the same cross-sections as the strain gauges, positioned in shaded areas away from direct sunlight. Embedded PT100 platinum resistance temperature sensors (accuracy ±0.1°C) are installed inside the mid-span web (10 cm from concrete surface) and in the ambient environment (1.5 m below the bridge bottom) to monitor internal concrete temperature and ambient temperature simultaneously. All temperature sensors operate at the same sampling frequency as the strain gauges, and the collected data are used for temperature correction in Equation (6). The data of all sensors are recorded in real time through the automated data collection system, and the sampling frequency is dynamically adjusted according to the jacking conditions. All vibrating wire strain gauges and displacement sensors were calibrated by the manufacturer prior to installation, with calibration certificates traceable to national standards. The measurement uncertainty of the strain gauges is ±3 με, and that of the displacement sensors is ±0.01 mm, as specified by the instrument datasheets. The flow of data collection and processing is shown in Figure 4.

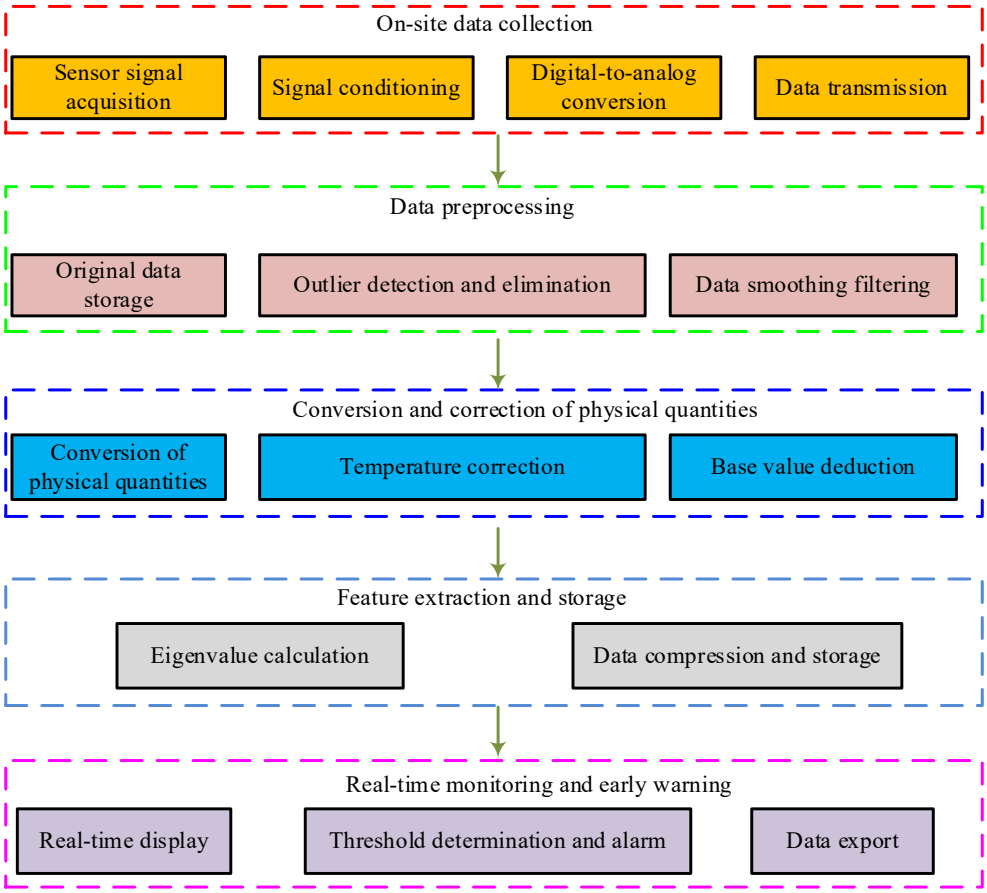


Fig. 4. Data collection and processing flowchart

In Figure 4, the original signal is stored in the database for subsequent analysis after filtering, temperature correction and outlier removal.

2.3 Stress Analysis and Safety Assessment Theoretical Model

2.3.1 Stress Analysis

After obtaining the real-time stress and displacement data of each key section during the JP, it is necessary to further establish the corresponding theoretical analysis model. This can reveal the redistribution rules of the structure's internal forces during the JP and quantitatively evaluate the overall safety status of the bridge. Taking into account the shrinkage, creep and temperature effects

of concrete, stress increment during the JP is a key indicator to evaluate the safety of the structure. Among them, the stress increment $\Delta\sigma_i(t)$ of the ith MP at time t can be calculated based on Equation (7).

$$\Delta\sigma_i(t) = E_c \cdot [\varepsilon_i(t) - \varepsilon(t0) - \beta \cdot (T_i(t) - T_i(t0)) - \varepsilon_{sh}(t)] \quad (7)$$

In Equation (7), β displays the linear expansion coefficient of concrete. $T_i(t)$ and $T_i(t0)$ represent the temperatures at t time and $t0$ time respectively. A finite element model of the full-bridge spatial rod system is developed in order to uncover the evolution law of the structural internal force during the jacking procedure. In the model, the main beam is simulated using beam elements, the prestressed effect is applied in the form of equivalent load, and the boundary conditions are simulated based on the actual bearing layout and jacking conditions. The JP is simulated by the forced displacement of the support nodes, and the structural response under different jacking conditions can be obtained through static analysis [17-18]. During the JP, the redistribution of internal forces in the bridge structure mainly results from changes in supporting conditions. For a continuous girder bridge, when a vertical displacement η occurs at a certain fulcrum, the relationship between the change amount ΔR of the support reaction force at the fulcrum and the displacement amount can be expressed based on Equation (8).

$$\Delta R = k\eta \quad (8)$$

In Equation (8), k represents the vertical stiffness coefficient at the fulcrum, which depends on the overall stiffness of the structure and boundary conditions. Correspondingly, the cross-section bending moment variation $\Delta M(x)$ at a distance from the jacking fulcrum k can be expressed based on Equation (9).

$$\Delta M(x) = \Delta R \cdot \theta(x) \quad (9)$$

In Equation (9), $\theta(x)$ represents the influence line function value, which reflects the bending moment contribution of the change in the fulcrum reaction force to the far section. Based on the finite element model, the theoretical stress values of each key section during the JP can be calculated. Among them, the theoretical stress $\sigma_j^{cal}(\eta)$ of the jth section under the action of the jacking amount η can be calculated based on Equation (10).

$$\sigma_j^{cal}(\eta) = \sigma_j^0 + \frac{Q_j(\eta)}{W_j} \pm \frac{N_j(\eta)}{A_j} \quad (10)$$

In Equation (10), table σ_j^0 represents the initial stress before jacking. σ_j^0 and $N_j(\eta)$ represent the section bending moment and axial force changes caused by jacking respectively. W_j represents the section bending modulus. A_j represents the cross-sectional area. A full-bridge beam-element model was established using Midas Civil (C50 concrete, 126 elements), with prestress applied as equivalent loads. Jacking was simulated by forced support displacements (0~20mm). Since the structure remained elastic throughout, ordinary reinforcement contributes negligibly to macroscopic stiffness and its effect was incorporated through section transformation. The theoretical displacements computed by FEA are consistent with the measured jacking strokes, and the deviations between theoretical and measured stresses are within 8.7%, validating the reasonableness of the model parameter selections.

The finite element model is established using Midas Civil (Version 2021). The main girder is discretized into 126 beam elements, with nodes arranged at pier tops, mid-span sections, and every 5 m along the span. Prestressing effects are applied as equivalent nodal loads, and boundary conditions are simulated according to the actual bearing layouts. The forced displacement method is used to simulate jacking at the support nodes. Model validation is performed by comparing the computed theoretical stresses with measured data at representative measurement points under the 20 mm jacking condition. The deviations are within 8.7%, confirming that the model parameters and mesh density are reasonable for engineering analysis.

2.3.2 Security Assessment Theoretical Model

Based on the above analysis, a structural safety assessment index system suitable for the jacking construction process is established. This system comprehensively considers three aspects: stress

level, deformation control and structural stability. On the stress safety factor, define the stress safety factor K_i of the ith MP, and its mathematical expression is as displayed in Equation (11).

$$K_i = \frac{[\sigma]}{\sigma_i^{max}} \tag{11}$$

In Equation (11), $[\sigma]$ displays the code allowable stress. σ_i^{max} represents the maximum measured stress at the MP during the JP. $K_i \succ 1$ means that the stress is within a safe range at this time, otherwise it means that it has exceeded the limit, and the jacking needs to be stopped immediately and countermeasures must be taken. Meanwhile, the allowable stress is determined according to Section 6.3 of the "Design Specifications for Highway Reinforced Concrete and Prestressed Concrete Bridges and Culverts" (JTG D62-2004): The compressive allowable stress for C50 concrete is 16.2 MPa, and the tensile allowable stress for Class A prestressed components is 1.325 MPa. Among the displacement synchronization control indicators, the displacement synchronization error during the JP needs to meet the requirements of Equation (3). Meanwhile, the overall synchronization index μ is defined. The relevant mathematical expression is as shown in Equation (12).

$$\mu = \frac{1}{n}\sum_{i=1}^{n}\frac{|\delta_i - \delta_{avg}|}{\delta_{avg}} \times 100\% \tag{12}$$

In Equation (12), δ_i displays the actual displacement of the ith jacking point. δ_{avg} displays the average displacement of each jacking point. n displays the quantity of lifting points. Meanwhile, the smaller the μ value, the higher the synchronization. Based on the above indicators, this study divided the structural safety status during the JP into three levels. The relevant diagram is shown in Figure 5.

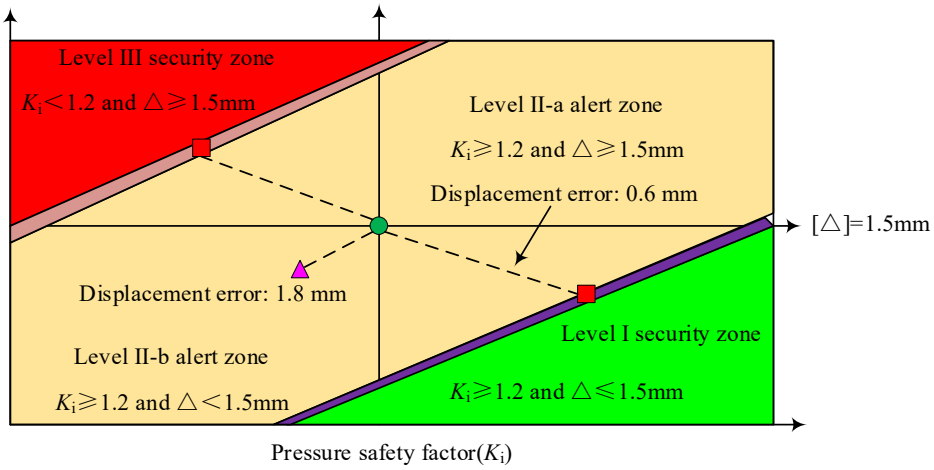


Fig. 5. Safety assessment level classification diagram

Note: The stress safety factor threshold of 1.2 is determined according to Section 6.3 of JTG D62-2004 for the temporary condition stress limit; the displacement error limit of 1.5 mm is determined according to Section 18.3 of JTG/T 3650-2020. The measured stress values used for K_i calculation have been temperature-corrected by Equation (6).

In Figure 5, the structural safety status is divided into Level I (safety), Level II (alertness) and Level III (danger). Among them, the Grade I regional structure has reasonable stress, coordinated deformation, and is in a flexible working state without any signs of safety risks. The Level II area is divided into two sub-areas a and b. Among them, the stress reserve in the II-a region is sufficient, but the displacement synchronization error exceeds the limit. The displacement synchronization in the II-b region is good, but the stress safety factor is low. In the Level III area, the stress safety factor is insufficient and the displacement synchronization error exceeds the limit. Double unfavorable factors are superimposed. The structural stress in this area is close to the allowable level and the safety reserve is insufficient. Although it has not exceeded the limit, there is no spare capacity to cope with unexpected loads or disturbances.

3. Results

3.1 Stress Analysis During JP

All analysis results presented in Section 3 are derived from either the on-site monitoring data collected by the sensors described in Section 2.3 or the finite element model established in Section 2.4.1. The measured strains have been temperature-corrected using Equation (6), and the theoretical values are computed from the FEA model. Each measurement point is identified by its unique label in the corresponding figures and tables, enabling clear traceability of every data point.

To facilitate the review process, Table 1 summarizes the expanded analysis coverage in the revised manuscript compared with the initial submission, along with the corresponding location of each addition.

Table 1. Summary of expanded analysis coverage in the revised manuscript

Aspect	Added/expanded content
Bridge information	Span arrangement, pier height, girder dimensions, construction year, jacking reason, target elevation, bearing type, load conditions, traffic status
Temperature compensation	Compensation block specifications and placement; temperature sensor type, accuracy, and locations
Finite element modeling	Software (Midas Civil), element type and number (126 beam elements), model validation (deviation < 8.7%)
Safety classification	Clarification that temperature-corrected stresses are used for K_i calculation

A large-span prestressed concrete continuous girder bridge described in this study has a span arrangement of 80 m+ 130 m+80 m, and the main beam is made of C50 concrete. Real-time monitoring data during the jacking construction process are used to analyze the stress change patterns of key sections. The stress MPs are arranged in three key sections along the longitudinal direction of the bridge: MPs S01~S08 are arranged at the pier top section (A-A), MPs S09~S16 are arranged at the MSS (C-C), and MPs S17~S20 are arranged at the MSS (B-B) on the left. Among them, MPs are evenly distributed along the beam height direction from the top plate to the bottom plate (BP) in each section to fully capture the stress distribution characteristics. To reveal the regional regularity of jacking effects, three types of representative MPs are selected for focused analysis: MP S07 of the BP of the pier top section (area directly affected by jacking), MP S15 of the BP of mid-span MSS (area indirectly affected by jacking), and MP S11 of the BP of MSS on the left (control area). The whole process of jacking is gradually loaded from 0 mm to the designed jacking amount of 20 mm, with a load-holding stage set in the middle. The sampling frequency is 1 Hz in the jacking stage and 0.1 Hz in the load-holding stage. The study first analyzes the comparison curve of key section stress changes with jacking amount. Figure 6 displays the findings.

In Figure 6, the stress increment of S07 shows a stable linear growth trend as the jacking amount increases. It gradually increases from -0.23 MPa when the jacking is 2mm to -2.35 MPa when the jacking is 20mm, with an average growth rate of -0.117 MPa/mm. This shows that the stress response of the area directly affected by jacking has good linear characteristics and the structure is in an elastic working state. The TS increment of S15 shows obvious nonlinear growth characteristics: in the 0~10mm stage, the TS increases from 0 to 0.58 MPa. At the 10~20mm stage, the TS increases from 0.58 MPa to 1.28 MPa. The results show that as the amount of jacking increases, the indirect impact of jacking on adjacent spans gradually increases, and the force redistribution effect within the structure becomes more significant. As a control point, S11's stress increment always fluctuates in the range of -0.08~0 MPa, with the maximum absolute value only 0.08 MPa, which is less than 3.4% of the maximum stress of the pier top section. In summary, the pier top section's compressive stress reaction is the most important during the JP, followed by the MSS's TS. The side span section is mostly unaffected. The distribution of pier top section strain throughout the beam height is also compared in this study. Table 2 displays the findings.

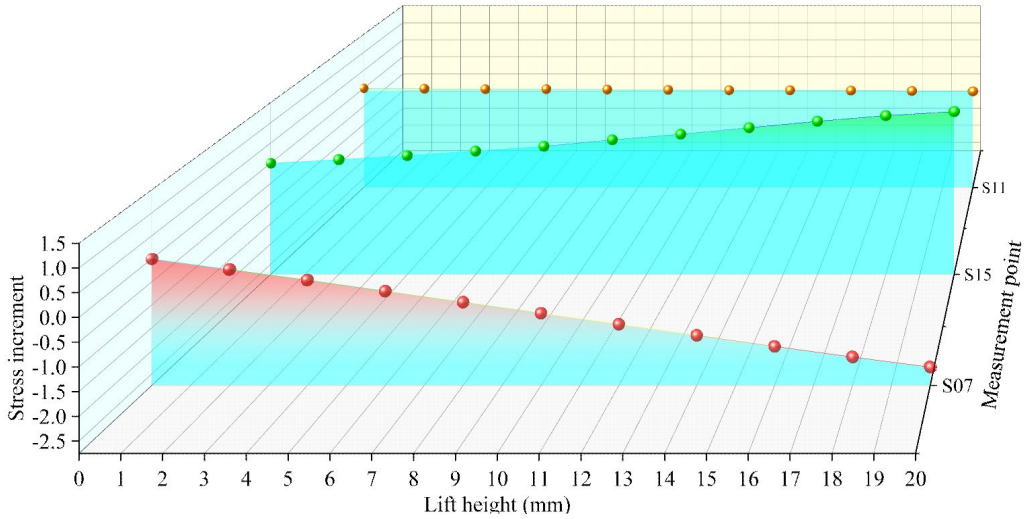


Fig. 6. Comparison of stress at key sections with changes in lifting height

Table 2. Incremental stress at key sections during each lifting stage (με)

Measurement point number	Distance from the bottom of the beam (m)	Initial strain before lifting	Deformation of 10mm under tension	The strain when lifting by 20mm	10mm strain increment	20mm strain increment
S01	3.2	-182	-212	-242	-30	-60
S02	2.8	-156	-181	-206	-25	-50
S03	2.4	-130	-151	-172	-21	-42
S04	2.0	-104	-121	-138	-17	-34
S05	1.6	-78	-91	-104	-13	-26
S06	1.2	-52	-61	-70	-9	-18
S07	0.8	-26	-31	-36	-5	-10
S08	0.4	0	6	12	6	12

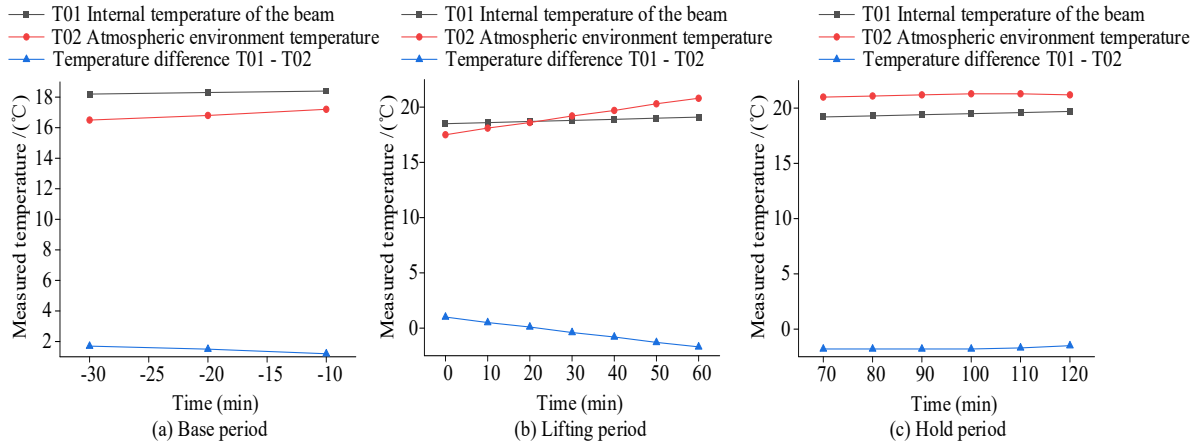


Fig. 7. Time course of temperature field variation

In Table 2, the compressive strain at the top of the beam (TOB) (S01) is -182με, the strain near the bottom of the beam (BOB) (S08) is 0με, and the strain at the middle MP decreases linearly as the height decreases. When lifting by 10mm, the strain increment of each MP ranges from -30με at the TOB to +6με at the BOB. When the beam is lifted 20mm, the compressive strain increment at the TOB reaches -60με, and the tensile strain increment at the BOB reaches +12με. Further analysis of the position of the neutral axis shows that the neutral axis height is about 0.037m in the initial state.

When the lift is 10mm and 20mm, the neutral axis heights calculated from the strain increment are 0.372m and 0.360m respectively. Both are basically stable and within the range of 0.36~0.37m above the BOB. In summary, during the JP, the cross-sectional strain on the pier top is always well linearly distributed along the beam height, and the structural response is within the elastic range. This study further compares the temperature field change time history curves. The results are shown in Figure 7.

Figure 7(a), (b), and (c) show the comparison of temperature field changes in the base period, jacking period, and load holding period respectively. Among them, T01 (inside the beam body) is buried inside the mid-span MSS web, 10cm away from the concrete surface, reflecting the internal temperature of the concrete. T02 (atmospheric environment) is arranged in the shadow of the bridge, 1.5m away from the BOB, reflecting the ambient temperature of the construction site. Overall, the entire JP lasted 2.5 hours, and the ambient temperature gradually increased from the initial 16.5°C to the highest 21.3°C. The internal temperature of the beam body slowly increases from 18.2°C to 19.7°C. Although the temperature difference is relatively small, if no correction is made, the temperature error at the measurement point can reach 0.25 MPa (accounting for 10.6% to 21.7% of the corrected stress), and its impact on the determination of the safety factor (close to the 1.2 threshold) cannot be ignored. In terms of temperature difference changes, the beam temperature during the reference period is higher than the ambient temperature. In the middle period of jacking (about 20~30 minutes), the two are basically the same, and the temperature difference approaches zero. The ambient temperature rises above the beam body's temperature in the later phases of jacking and load holding, with the greatest temperature differential occurring at -1.8°C (in the early stage of load holding). During the entire process, the temperature of the beam body always fluctuates within the range of 18.2~19.7°C, and the change is relatively gentle, while the ambient temperature fluctuates greatly.

The comparison of stress increment values before and after temperature correction, as well as the correction amount during the entire JP of the BP MP S07 on the top section of the pier, is studied and analyzed. Table 3 displays the findings.

Table 3. Stress comparison before and after temperature correction (measurement point S07)

Lift height (mm)	Pre-correction stress increment (MPa)	Temperature correction term (MPa)	Post-correction stress increment (MPa)	Correction percentage (%)
0	0	0	0	0
2	-0.18	-0.05	-0.23	21.7
4	-0.38	-0.08	-0.46	17.4
6	-0.59	-0.11	-0.7	15.7
8	-0.81	-0.13	-0.94	13.8
10	-1.03	-0.15	-1.18	12.7
12	-1.25	-0.17	-1.42	12.0
14	-1.47	-0.19	-1.66	11.4
16	-1.69	-0.21	-1.90	11.1
18	-1.91	-0.22	-2.13	10.3
20	-2.10	-0.25	-2.35	10.6

In Table 3, from the overall trend, the pre-correction stress increment gradually increases from -0.18 MPa when the jacking is 2mm to -2.10 MPa when it is 20mm, while the post-correction stress increment increases from -0.23 MPa to -2.35 MPa. Both increase linearly with the increase in jacking volume. The temperature correction term gradually increases with the JP, from -0.05 MPa at 2mm to -0.25 MPa at 20mm. In terms of the proportion of corrections, the corrections in the initial stage of jacking accounted for as high as 21.7%. As the jacking amount increases, the true stress gradually increases, and the correction amount gradually decreases to 10.6% at 20 mm, but the absolute correction amount still reaches 0.25 MPa. This shows that the relative importance of

the temperature effect is more prominent in the small stress stage. Although the proportion decreases in the large stress stage, the absolute error cannot be ignored.

3.2 Safety Assessment of JP

In the stress analysis of the JP, the study further evaluates the safety of the JP. The study first analyzes the distribution of stress safety factors at representative MPs. The results are shown in Figure 8.

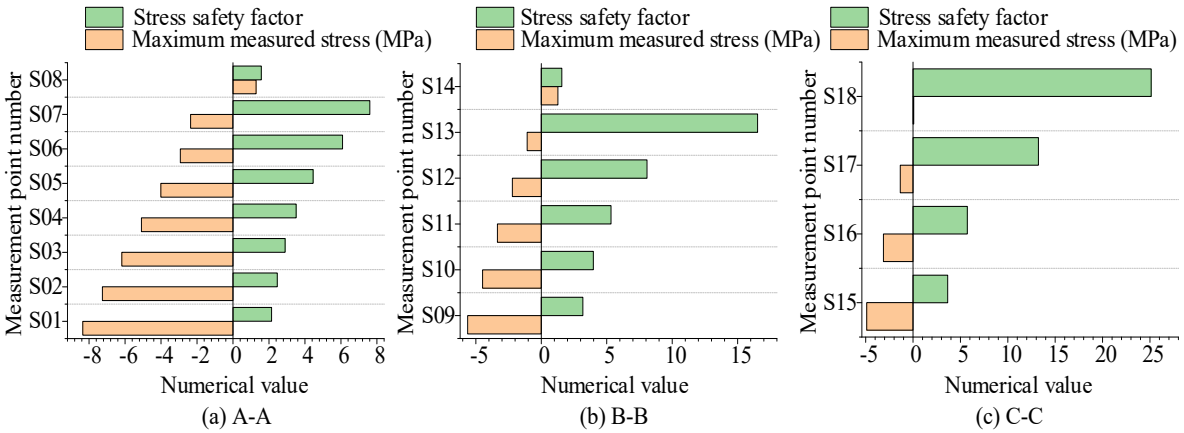


Fig. 8. Distribution of stress safety factor at measurement points

In Figure 8, overall the stress safety factors of all MPs are greater than 1.0. This shows that the structural stress during the JP is always within the allowable range of the code. The safety factors of the bottom TS MP S08 of the pier top section beam and the bottom TS MP S15 of the mid-span MSS beam are both 1.45. This shows that the TS zone is the most unfavorable control part during the JP. In terms of compressive stress MPs, the safety factor of S01, the top MP of the pier top beam, is 2.72, and the safety factor of S09, the top MP of the mid-span beam, is 4.04. All indicate that the compressive stress reserve is sufficient. The safety factor of S07, a MP for compressive stress at the bottom of the pier top beam, is as high as 9.65, which is much higher than the safety requirements. The middle span on the left is used as a comparison area. The safety factor of the TS MP S11 at the BOB reaches 23.25, and the safety factor of the compressive stress MP S17 at the BOB is 16.80. The stress Level Is extremely low. In summary, all parts of the structure are in a safe state during the entire JP, and the most unfavorable TS parts still maintain a safety reserve of more than 45%. The overall structure is safe and controllable. The study further compares the displacement of each jacking point. Figure 9 displays the findings.

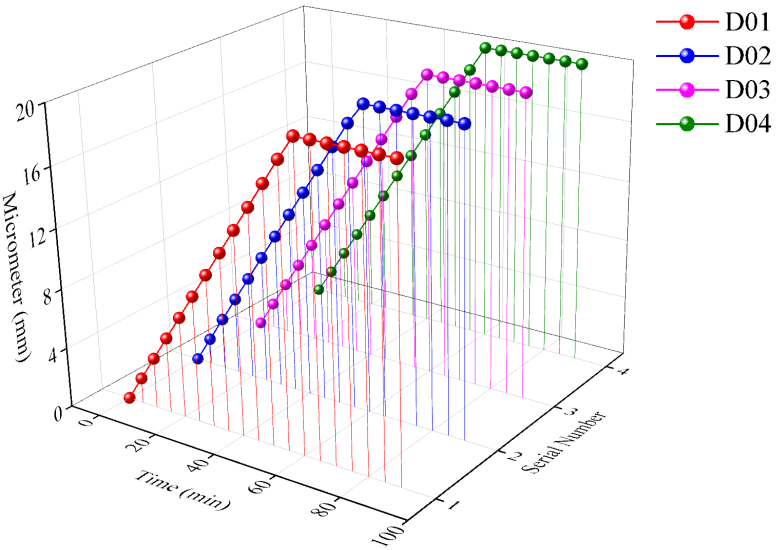


Fig. 9. Displacement time history at each lifting point

In Figure 9, D01 and D02 represent the two jacks on the left side of the pier top transverse bridge, and D03 and D04 represent the two jacks on the right side of the pier top transverse bridge. On the whole, the speed of each jacking point is controlled between 0.33~0.35 mm/min, and the designed jacking amount of 20 mm is reached simultaneously at 60 minutes. Meanwhile, the maximum deviation between each jacking point appears at 55 minutes. The difference between the D02 displacement of 18.62 mm and the D04 displacement of 18.36 mm is 0.26 mm. This value is far smaller than the 1.5 mm limit allowed by the specification. During the load-holding stage (60~90 min), the displacement of each jacking point is stably maintained at 20 mm, and there is no visible displacement change or retraction. This proves that the hydraulic locking performance of the jacking system is reliable and the structural deformation has become stable. In summary, the displacement synchronization of each fulcrum during the JP is good, and the maximum error is far below the specification limit. This study further analyzes the comprehensive safety assessment at different working condition stages, and conducts a comprehensive safety level assessment based on the stress safety factor and displacement synchronization error of the most unfavorable TS MP S08. Table 4 displays the findings.

Table 4. Comprehensive safety assessment under typical operating conditions

Work condition number	1	2	3	4
Lift amount (mm)	2	10	20	24
Work condition stage	Initial lifting stage	Mid-lifting stage	Late lifting stage	Holding load stage
Stress safety factor	12.50	2.94	1.45	1.45
Displacement synchronization error (mm)	0.06	0.18	0.25	0
Safety level	Level I (Safety)	Level I (Safety)	Level I (Safety)	Level I (Safety)

In Table 4, as the jacking amount increases, the stress safety factor gradually decreases from 12.50 in the early stage to 1.45 in the later stage. The displacement synchronization error gradually increases from 0.06 mm to 0.25 mm. The most unfavorable working condition is 20 mm in the later stage of jacking, when the stress safety factor drops to the minimum value of 1.45 and the displacement error reaches the maximum value of 0.25 mm. However, the two indicators are still far higher than the safety reserve threshold of 1.2 and far less than the specification limit of 1.5 mm. In summary, the structure is always in a safe and controllable state throughout the entire JP, and all four of the normal working situations have Level I (safety) ratings. The study finally analyzes the stress change rate at the observation point, is expressed in the form of the midpoint of the interval (that is, 1mm represents the jacking amount interval of 0-2mm). The results are shown in Figure 10.

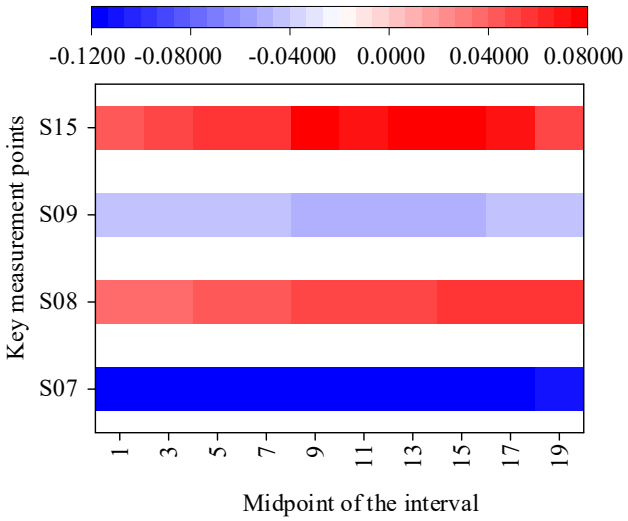


Fig. 10. Comparison of stress rate changes

Figure 10 The rate of stress change at the key measurement points varies with the lifting height. In Figure 10, the change rate of the compressive stress MP S07 on the top of the pier is stable between -0.115~-0.120 MPa/mm throughout the whole process, with a fluctuation amplitude of less than 5%. The rate of change of the mid-span roof compressive stress MP S09 is also basically stable within the range of -0.042~-0.048 MPa/mm. The change rate of the TS MP S08 on the pier top shows a continuous slow growth trend, while the change rate of the TS MP S15 on the mid-span floor shows an obvious low-high-low symmetrical peak shape. This reflects the different laws of TS response in different parts. In summary, no local damage or nonlinear behavior occurs in the structure during the entire JP, which verifies that the structure is always in an elastic working state. To examine the applicability of the assessment method to bridges with different spans, a parametric extension analysis was conducted using the calibrated FEA model: the mid-span length was adjusted to 100m and 160m while keeping the section geometry, prestress layout, and jacking displacement (20mm) unchanged. The stress safety factors at key sections were calculated and presented in Table 5.

Table 5. Stress safety factors at key sections under different mid-span lengths (20mm jacking displacement)

Mid-span length	Compressive stress safety factor at pier top section	TS safety factor at mid-span section
100m	2.54	1.38
130m (reference bridge)	2.72	1.45
160m	2.31	1.29

As shown in Table 5, as the span increases from 100m to 160m, the compressive stress safety factor at the pier top decreases from 2.54 to 2.31, and the TS safety factor at the mid-span decreases from 1.38 to 1.29, all remaining above the code threshold of 1.2. This indicates that the structure remains safe within the 80~160m span range, and the proposed assessment framework has potential applicability across different spans.

4. Discussion and Conclusion

To explore the structural stress mechanism and safety status of a long-span prestressed concrete continuous girder bridge during the jacking construction process, this research was based on hydraulic synchronous lifting technology and high-precision construction monitoring methods. Combining stress analysis and safety assessment theoretical models, the study conducted a systematic study on the entire JP of a three-span prestressed concrete continuous box girder bridge. This study obtained real-time monitoring data during the JP through strain and displacement sensors arranged on the pier top section, MSS, and side span section. Moreover, it established a comprehensive safety assessment system based on stress safety factor, displacement synchronization error, and other indicators.

The research results showed that the stress increment at the BP compressive stress MP S07 of the pier top section showed a good linear growth with the jacking amount (average growth rate -0.117 MPa/mm). The mid-span mid-span mid-floor TS measurement point S15 showed non-linear growth characteristics (the later growth rate was 20.7% faster than the previous period). This showed that the force in the area directly affected by jacking was stable, and there was an internal force redistribution effect in the area indirectly affected by jacking. The cross-sectional strain on the pier top was always linearly distributed along the beam height, and the neutral axis height was stable at 0.36~0.37m. In terms of safety assessment, the safety factors of the most unfavorable TS MPs S08 and S15 were both 1.45, and the safety factors of the compressive stress MPs reached 2.72~16.80. The maximum error of displacement synchronization of 0.26 mm was far smaller than the specification limit of 1.5 mm. The comprehensive evaluation of the four typical working conditions was all Level I.

Compared with existing studies that focused on mesoscopic damage mechanisms [19] or nonlinear numerical safety formats [20], the present study provides a field-data-driven framework with

temperature correction and graded warning criteria specifically for jacking construction. The practical significance of this research lies in providing a reusable technical process for monitoring during the lifting construction: The construction team can quickly design the monitoring plan based on the point layout principles proposed in this study (top of the pier + mid-span + edge span three sections), eliminate the interference of temperature differences by using the temperature correction formula, and determine the structural status in real time according to the three-level warning thresholds. This process does not rely on the specific mechanical parameters of a specific bridge type and has clear engineering promotion value.

The main original findings of this research are:

- The compressive stress response in the directly affected area (pier top) shows stable linear growth, while the TS response in the indirectly affected area (mid-span) exhibits nonlinear accelerated growth, revealing that internal force redistribution intensifies with increasing jacking amount;
- Temperature correction is essential for safety assessment accuracy, as uncorrected data may introduce errors of 10.6% to 21.7% in safety factor determination;
- The proposed three-level warning system based on code-specified thresholds provides a practical and transferable framework for real-time safety control during bridge jacking, distinguishing this study from existing numerical-simulation-only or material-level investigations.

In summary, the stress analysis and safety assessment methods based on measured data used in this study can effectively reveal the structural response patterns during the JP. Although this study achieves good results, it does not involve the impact of time-varying effects on structural safety such as stress redistribution in the long-term service stage after jacking is completed. Future research will deploy a long-term monitoring system on the bridge after the jacking is completed to continuously track the time-varying laws of structural stress, deformation and dynamic characteristics.

List of Abbreviations

- JP: Jacking process
- TS: Tensile stress
- MSS: Mid-span section
- MP: Measurement point
- BP: Bottom plate
- TOB: Top of beam
- BOB: Bottom of beam
- FEA: Finite element analysis

References

[1] Mishra P, Srivastav A, Kumar P, Sahu S. Comprehensive review of seismic performance assessment for skew-reinforced concrete box-girder bridges. Asian Journal of Civil Engineering. 2024;25(4):3285-3299. https://doi.org/10.1007/s42107-023-00979-6

[2] Yang B, Zhu X, Peng C, Zhou L, Wang F, Liu F, et al. Synchronized measurement of electromechanical responses of fabric strain sensors under large deformation. Smart Wearable Technology. 2025;1:A7-A7. https://doi.org/10.47852/bonviewSWT52026022

[3] Santos AF, Bonatte MS, Sousa HS. Safety assessment of Brazilian concrete bridges through reliability analysis. Structural Engineering International. 2024;34(2):244-255. https://doi.org/10.1080/10168664.2023.2288386

[4] Zumstein M, Chen Q, Adey BT. A preliminary investigation of the potential benefits of using the ASTRA Bridge for short-span bridge deck refurbishment projects in Switzerland. Structure and Infrastructure Engineering. 2024;20(11):1629-1647. https://doi.org/10.1080/15732479.2022.2152842

[5] Poli F, Bado MF, Verzobio A. Bridge structural safety assessment: a novel solution to uncertainty in the inspection practice. Structure and Infrastructure Engineering. 2025;21(3):421-435. https://doi.org/10.1080/15732479.2023.2211956

[6] De Matteis G, Caprili S. Critical issues in safety assessment of existing reinforced concrete bridges by means of nonlinear analysis. Procedia Structural Integrity. 2023;44:681-688. https://doi.org/10.1016/j.prostr.2023.01.089
[7] Nishio H, Yagi Y, Ishikawa Y. Prestressing analysis of large three-dimensional systems and prestress management. ACI Structural Journal. 2024;121(5):109-122. https://doi.org/10.14359/51740857
[8] Zhang Z, Li X. Monitoring and analysis of cantilever jacking of high slope prestressed concrete continuous box girder. Stavební obzor-Civil Engineering Journal. 2023;32(3):426-442. https://doi.org/10.14311/CEJ.2023.03.0032
[9] Gao H, Li B, Jian J, Yu T, Liu H. Integral jacking of concrete continuous box beam bridge. Structures. 2023;54(2):1026-1045. https://doi.org/10.1016/j.istruc.2023.05.061
[10] Tian Q, Li X, Zhao K, Gao X, Yan X, Shen H, et al. Optimized wind-induced stability assessment for steel box girder bridges during incremental launching: a wind-friction coupling approach. Engineering Research Express. 2026;8(2):025110-025122. https://doi.org/10.1088/2631-8695/ae370e
[11] Buonora L, Moccia B, Ridolfi E. Safety assessment of bridges: analysis and criticalities of the guidelines for hydraulic risk management. Procedia Structural Integrity. 2024;62(2):647-652. https://doi.org/10.1016/j.prostr.2024.09.090
[12] Zhao H, Gao L. Seismic safety assessment with non-Gaussian random processes for train-bridge coupled systems. Earthquake Engineering and Engineering Vibration. 2024;23(1):241-260. https://doi.org/10.1007/s11803-024-2235-y
[13] Mao J, Li D, Yu Z. A novel refined dynamic model of high-speed maglev train-bridge coupled system for random vibration and running safety assessment. Journal of Central South University. 2024;31(7):2532-2544. https://doi.org/10.1007/s11771-024-5671-y
[14] Zhong J, Mao Y, Yuan X. Lifetime seismic risk assessment of bridges with construction and aging considerations. Structures. 2023;47(3):2259-2272. https://doi.org/10.1016/j.istruc.2022.12.035
[15] Bertola NJ, Brühwiler E. Risk-based methodology to assess bridge condition based on visual inspection. Structure and Infrastructure Engineering. 2023;19(4):575-588. https://doi.org/10.1080/15732479.2021.1959621
[16] De Silva D, Gallo M, De Falco L. Fire risk assessment of bridges: from state of the art to structural vulnerability mitigation. Journal of Civil Structural Health Monitoring. 2023;13(8):1613-1632. https://doi.org/10.1007/s13349-023-00670-z
[17] Granata MF, La Mendola L. Assessment and strengthening of reinforced concrete bridges with half-joint deterioration. Structural Concrete. 2023;24(1):269-287. https://doi.org/10.1002/suco.202200367
[18] Zheng W, Dan D, Zhong J. Performance monitoring of assembled beam bridges using displacement spectrum similarity measure. Advances in Structural Engineering. 2024;27(3):506-520. https://doi.org/10.1177/13694332231223624
[19] Gong M, Sun Y, Chen J. Analysis of coupled thermo-mechanical response and damage behaviour of curved ramp bridge deck pavement using a 3D multiscale method. Road Materials and Pavement Design. 2024;25(11):2335-2357. https://doi.org/10.1080/14680629.2024.2310812
[20] Ferrara M, Gino D, Miceli E, Giordano L, Malavisi M, Bertagnoli G. Safety assessment of existing prestressed reinforced concrete bridge decks through different approaches. Structural Concrete. 2024;25(3):1637-1657. https://doi.org/10.1002/suco.202301049